

Production of a_1 in heavy meson decays

Wei Wang^{1,2,a}, Zhen-Xing Zhao^{1,b}

¹ INPAC, Shanghai Key Laboratory for Particle Physics and Cosmology, Department of Physics and Astronomy, Shanghai Jiao-Tong University, Shanghai 200240, China

² State Key Laboratory of Theoretical Physics, Institute of Theoretical Physics, Chinese Academy of Sciences, Beijing 100190, China

Received: 23 November 2015 / Accepted: 18 January 2016 / Published online: 3 February 2016
© The Author(s) 2016. This article is published with open access at Springerlink.com

Abstract In this work, we study various decays of heavy B/D mesons into the $a_1(1260)$, based on the form factors derived in different nonperturbative or factorization approaches. These decay modes are helpful to explore the dynamics in the heavy to light transitions. Meanwhile they can also provide insights to a newly discovered state, the $a_1(1420)$ with $I^G(J^{PC}) = 1^-(1^{++})$ observed in the $\pi^+ f_0(980)$ final state in the $\pi^- p \rightarrow \pi^+ \pi^- \pi^- p$ process. Available theoretical explanations include tetraquark or rescattering effects due to $a_1(1260)$ decays. If the $a_1(1420)$ were induced by the rescattering, its production rates are completely determined by those of the $a_1(1260)$. Our numerical results for decays into the $a_1(1260)$ indicate that there is a promising prospect to study these decays on experiments including BES-III, LHCb, Babar, Belle, and CLEO-c, the forthcoming Super-KEKB factory and the under-design Circular Electron-Positron Collider.

1 Introduction

Since Gell-Mann proposed the concept of quarks in 1964 [1], quark model has achieved indisputable successes: most of the established mesons and baryons on experimental side can be well accommodated in the predicted scheme [2]. However, recently there have been experimental observations of resonance-like structures with quantum numbers hardly to be placed in the quark-antiquark or three-quark schemes [3–9]. This leads one to the suspect that the hadron spectrum is much richer than the simple quark model [10].

In the quark model, the possible quantum numbers J^{PC} for orbitally excited axial-vector mesons are 1^{++} or 1^{+-} , depending on different spin couplings of the two quarks. Heavy meson decays offer a promising opportunity to investigate these axial-vector mesons. Since the observation of the

$B \rightarrow J/\psi K_1$ [11] and $D^* a_1(1260)$ [12] decays, there are increasing experimental studies on B meson decays involving a p-wave axial-vector meson in the final state [13]. One purpose of this work is to provide the theoretical results for branching ratios of various B or D decays into the $a_1(1260)$. As we will show later, the results are very different in distinct nonperturbative or factorization approaches, and thus measurements in the future may be capable to clarify these differences. Some previous theoretical studies can be found in the literature [14–25].

Recently the COMPASS collaboration [26, 27] has reported the observation of a light resonance-like state with quantum numbers $I^G(J^{PC}) = 1^-(1^{++})$ in the P -wave $f_0(980)\pi$ final state with $f_0(980) \rightarrow \pi^+ \pi^-$. The signal was also confirmed by the VES experiment [28] in the $\pi^- \pi^0 \pi^0$ final state. The new state was tentatively called $a_1(1420)$ with the mass $m_{a_1} \approx 1.42$ GeV and width $\Gamma_{a_1} \approx 0.14$ GeV. The interpretation of this state as a new $\bar{q}q$ meson is challenging, since it could hardly be accommodated as the radial excitation of the $a_1(1260)$, which is expected to have a mass above 1650 MeV. Therefore, this state has been interpreted as a tetraquark [29] or some dynamical effects arising from final state interactions [30, 31]. An illustration of the rescattering mechanism is shown in Fig. 1.

The deciphering of the internal structure of the $a_1(1420)$ can proceed not only through the detailed analysis of the pole position, but also through the decay and production characters. In this work, we propose that semileptonic and nonleptonic heavy meson decays can be used to examine the rescattering interpretation. In particular, an intriguing property in the rescattering picture is that the production rates of $a_1(1420)$ are completely determined by those of the $a_1(1260)$. In this case, the ratios

$$R(B \rightarrow a_1 X) = \frac{\mathcal{B}(B \rightarrow a_1^\pm(1420)X)\mathcal{B}(a_1^\pm(1420) \rightarrow f_0(980)\pi^\pm)}{\mathcal{B}(B \rightarrow a_1^\pm(1260)X)\mathcal{B}(a_1^\pm(1260) \rightarrow 2\pi^\pm\pi^\mp)}, \quad (1)$$

^a e-mail: wei.wang@sjtu.edu.cn

^b e-mail: zhaozx15@163.com

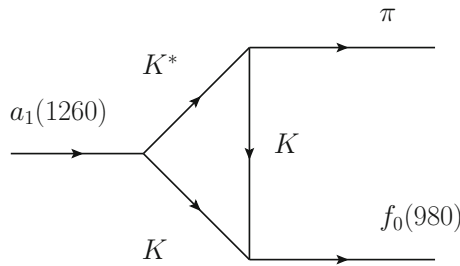


Fig. 1 Illustration of the $a_1^\pm(1260) \rightarrow \pi^\pm f_0(980)$

$$R(D \rightarrow a_1 Y) = \frac{\mathcal{B}(D \rightarrow a_1^\pm(1420) Y) \mathcal{B}(a_1^\pm(1420) \rightarrow f_0(980) \pi^\pm)}{\mathcal{B}(D \rightarrow a_1^\pm(1260) Y) \mathcal{B}(a_1^\pm(1260) \rightarrow 2\pi^\pm \pi^\mp)}, \quad (2)$$

would be insensitive to the production mechanism, and reduced to a constant. In the above equations, the X, Y correspond to certain leptonic/hadronic final states, and more explicitly we suggest to study in the charm sector the $D \rightarrow a_1 \ell^+ \nu$ and $D^0 \rightarrow \pi^\pm a_1^\mp$, and in the bottom sector the $B \rightarrow a_1 \ell^- \bar{\nu}$, $B \rightarrow D a_1, \pi^\pm a_1^\mp$, the $B_c \rightarrow J/\psi a_1$ and $\Lambda_b \rightarrow \Lambda_c a_1$ decays. The value for the ratios is estimated to be at percent level in Ref. [30]. Testing the universality of these ratios is a straightforward way to substantiate the rescattering interpretation.

The rest of this paper is organized as follows. In Sect. 2, we will concentrate on the $B \rightarrow a_1(1260)$ decays, including the transition form factors, semileptonic and nonleptonic decay modes. We will subsequently discuss the production of the $a_1(1260)$ in semileptonic and nonleptonic D/D_s decays in Sect. 3. The last section contains our summary.

2 B decays into a_1

2.1 Form factors

Unless specified in the following, we will use the abbreviation a_1 to denote the $a_1(1260)$ for simplicity. The Feynman diagram for semileptonic $\bar{B}^0 \rightarrow a_1^+ \ell^- \bar{\nu}$ decays is given in Fig. 2. After integrating out the off-shell W boson, one obtains the effective Hamiltonian

$$\mathcal{H}_{\text{eff}} = \frac{G_F}{\sqrt{2}} V_{ub} [\bar{u} \gamma_\mu (1 - \gamma_5) b] [\bar{\ell} \gamma^\mu (1 - \gamma_5) \nu_\ell]. \quad (3)$$

Here the V_{ub} is the CKM matrix element, and G_F is the Fermi constant.

Hadronic effects are parametrized in terms of the $B \rightarrow a_1$ form factors:

$$\langle a_1(p_{a_1}, \epsilon) | \bar{u} \gamma^\mu \gamma_5 b | \bar{B}(p_B) \rangle$$

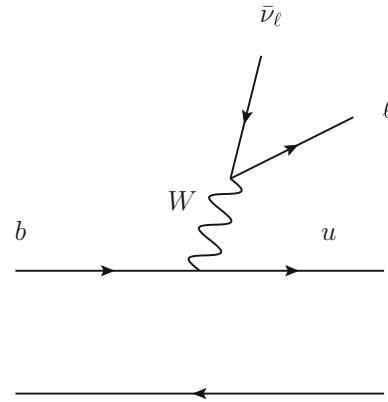


Fig. 2 Feynman diagram for the semileptonic $B \rightarrow a_1 \ell \bar{\nu}$ decay

$$\begin{aligned} &= -\frac{2i A(q^2)}{m_B - m_{a_1}} \epsilon^{\mu\nu\rho\sigma} \epsilon_\nu^* p_{B\rho} p_{a_1\sigma}, \\ &\langle a_1(p_{a_1}, \epsilon) | \bar{u} \gamma^\mu b | \bar{B}(p_B) \rangle \\ &= -2m_{a_1} V_0(q^2) \frac{\epsilon^* \cdot q}{q^2} q^\mu - (m_B - m_{a_1}) V_1(q^2) \\ &\quad \times \left[\epsilon^{*\mu} - \frac{\epsilon^* \cdot q}{q^2} q^\mu \right] + V_2(q^2) \frac{\epsilon^* \cdot q}{m_B - m_{a_1}} \\ &\quad \times \left[(p_B + p_{a_1})^\mu - \frac{m_B^2 - m_{a_1}^2}{q^2} q^\mu \right], \quad (4) \end{aligned}$$

with $q = p_B - p_{a_1}$, and $\epsilon^{0123} = +1$.

The $B \rightarrow a_1(1260)$ form factors have been studied in the covariant light-front quark model (LFQM) [14], light-cone sum rules (LCSR) [15] and perturbative QCD approach (PQCD) [16]. The corresponding results are collected in Table 1. In order to access the form factors in the full kinematics region, one has adopted the dipole parametrization [14–16]:

$$F(q^2) = \frac{F(0)}{1 - a(q^2/m_B^2) + b(q^2/m_B^2)^2}. \quad (5)$$

In the PQCD approach [16], the form factor V_2 is parametrized as

$$V_2(q^2) = \frac{1}{\eta} [(1 - r_{a_1})^2 V_1(q^2) - 2r_{a_1} (1 - r_{a_1}) V_0(q^2)]. \quad (6)$$

with $\eta = 1 - q^2/m_B^2$, and $r_{a_1} = m_{a_1}/m_B$.

From Table 1, we can see the three approaches, LFQM, LCSR, and PQCD, give very different results for the form factors and accordingly for branching fractions as we will show later. In the light-front quark model, a hadron is formed by the constituent quarks with the distribution in momentum space described by light-front wave functions, while the transition form factors are expressed as the overlap of two wave functions. In this framework, there is not hard-gluon exchange at the leading order in α_s . The LCSR starts from the quark-hadron duality, and can express the form factors

Table 1 Results for the $B \rightarrow a_1(1260)$ form factors calculated in the covariant light-front quark model (LFQM) [14], light-cone sum rules (LCSR) [15] and perturbative QCD approach (PQCD) [16]

$F(0)$	LFQM	LCSR	PQCD	a	LFQM	LCSR	PQCD	b	LFQM	LCSR	PQCD
A	0.25	0.48 ± 0.09	$0.26^{+0.06+0.00+0.03}_{-0.05-0.01-0.03}$	A	1.51	1.64	$1.72^{+0.05}_{-0.05}$	A	0.64	0.986	$0.66^{+0.07}_{-0.06}$
V_0	0.13	0.30 ± 0.05	$0.34^{+0.07+0.01+0.08}_{-0.07-0.02-0.08}$	V_0	1.71	1.77	$1.73^{+0.05}_{-0.06}$	V_0	1.23	0.926	$0.66^{+0.06}_{-0.08}$
V_1	0.37	0.37 ± 0.07	$0.43^{+0.10+0.01+0.05}_{-0.09-0.01-0.05}$	V_1	0.29	0.645	$0.75^{+0.05}_{-0.05}$	V_1	0.14	0.250	$-0.12^{+0.05}_{-0.02}$
V_2	0.18	0.42 ± 0.08	$0.13^{+0.03+0.00+0.00}_{-0.03-0.01-0.00}$	V_2	1.14	1.48	–	V_2	0.49	1.00	–

as a convolution of the hard kernel with the light-cone distribution amplitudes of the light hadron in the final state. The dominant contributions are also soft-overlapping type, and the most essential inputs are the LCDA of the a_1 meson. The PQCD approach is based on the k_T factorization, in which the soft-overlapping contributions are suppressed by the Sudakov factor. This guarantees the perturbative nature since the dominant contributions are from the hard-gluon exchange.

The fact that the three methods provide dramatically different predictions strongly calls for the clarification on experimental side. We believe the future measurements of various decays into the a_1 , especially semileptonic $B \rightarrow a_1 \ell \bar{\nu}$ decays including the differential decay distributions, are capable to accomplish this goal.

2.2 Semileptonic $\bar{B}^0 \rightarrow a_1^+(1260)\ell^-\bar{\nu}_\ell$ decays

Decay amplitudes for the $\bar{B}^0 \rightarrow a_1^+(1260)\ell^-\bar{\nu}_\ell$ can be divided into hadronic and leptonic sectors. Each of them are expressed in terms of the Lorentz invariant helicity amplitudes. The hadronic amplitude is obtained by evaluating the matrix element:

$$i\mathcal{A}_\lambda^1 = \sqrt{N_{a_1}} \frac{iG_F}{\sqrt{2}} V_{ub} \epsilon_\mu^*(h) \langle a_1 | \bar{u} \gamma^\mu (1 - \gamma_5) b | \bar{B} \rangle, \tag{7}$$

with $\hat{m}_l = m_l / \sqrt{q^2}$, $\beta_l = (1 - m_l^2/q^2)$, and

$$N_{a_1} = \frac{8}{3} \frac{\sqrt{\lambda} q^2 \beta_l^2}{256\pi^3 m_B^3}, \quad \lambda \equiv \lambda(m_B^2, m_{a_1}^2, q^2) = (m_B^2 + m_{a_1}^2 - q^2)^2 - 4m_B^2 m_{a_1}^2. \tag{8}$$

In the above, $\epsilon_\mu(h)$ with $h = 0, \pm, t$ is an auxiliary polarization vector for the lepton pair system. The polarized decay amplitudes are evaluated as

$$i\mathcal{A}_0^1 = -\sqrt{N_{a_1}} \frac{N_1 i}{2m_{a_1} \sqrt{q^2}} \left[(m_B^2 - m_{a_1}^2 - q^2)(m_B - m_{a_1}) \times V_1(q^2) - \frac{\lambda}{m_B - m_{a_1}} V_2(q^2) \right],$$

$$i\mathcal{A}_\pm^1 = \sqrt{N_{a_1}} N_1 i$$

$$\times \left[(m_B - m_{a_1}) V_1(q^2) \mp \frac{\sqrt{\lambda}}{m_B - m_{a_1}} A(q^2) \right], \tag{9}$$

$$i\mathcal{A}_t^1 = -i\sqrt{N_{a_1}} N_1 \frac{\sqrt{\lambda}}{\sqrt{q^2}} V_0(q^2), \tag{10}$$

with $N_1 = iG_F V_{ub} / \sqrt{2}$. For the sake of convenience, we use

$$i\mathcal{A}_{\perp/\parallel}^1 = \frac{1}{\sqrt{2}} [i\mathcal{A}_+^1 \mp i\mathcal{A}_-^1],$$

$$i\mathcal{A}_\perp^1 = -i\sqrt{N_{a_1}} \sqrt{2} N_1 \frac{\sqrt{\lambda} A(q^2)}{m_B - m_{a_1}},$$

$$i\mathcal{A}_\parallel^1 = i\sqrt{N_{a_1}} \sqrt{2} N_1 (m_B - m_{a_1}) V_1(q^2). \tag{11}$$

The differential decay width for $\bar{B}^0 \rightarrow a_1^+ \ell^- \bar{\nu}_\ell$ is then derived as

$$\frac{d\Gamma}{dq^2} = \frac{3}{8} \left[2I_1 - \frac{2}{3} I_2 \right], \tag{12}$$

with the I_i having the form

$$I_1 = [(1 + \hat{m}_l^2) |\mathcal{A}_0^1|^2 + 2\hat{m}_l^2 |\mathcal{A}_t^1|^2] + \frac{3 + \hat{m}_l^2}{2} [|\mathcal{A}_\perp^1|^2 + |\mathcal{A}_\parallel^1|^2],$$

$$I_2 = -\beta_l |\mathcal{A}_0^1|^2 + \frac{1}{2} \beta_l (|\mathcal{A}_\perp^1|^2 + |\mathcal{A}_\parallel^1|^2). \tag{13}$$

With the above formulas at hand, we present our results for differential branching ratios $d\mathcal{B}/dq^2$ (in units of $10^{-4}/\text{GeV}^2$) in Fig. 3. The left and right panels correspond to $\ell = (e, \mu)$ and $\ell = \tau$, respectively. The dotted, dashed, and solid curves are obtained using the LFQM [14], LCSR [15] and PQCD [16] form factors. The other input parameters are taken from the Particle Data Group (PDG) [2] as follows:

$$m_B = 5.28 \text{ GeV}, \quad \tau_{B^0} = 1.52 \times 10^{-12} \text{ s}, \quad m_{a_1} = 1.23 \text{ GeV},$$

$$m_e = 0.511 \text{ MeV}, \quad m_\mu = 0.106 \text{ GeV}, \quad m_\tau = 1.78 \text{ GeV},$$

$$G_F = 1.166 \times 10^{-5} \text{ GeV}^{-2}, \quad |V_{ub}| = (3.28 \pm 0.29) \times 10^{-3}. \tag{14}$$

As for the $|V_{ub}|$, we have quoted the value extracted from the exclusive $B \rightarrow \pi \ell \bar{\nu}_\ell$ for self-consistence; see Refs. [32,33] for discussions on the so-called $|V_{ub}|$ puzzle.

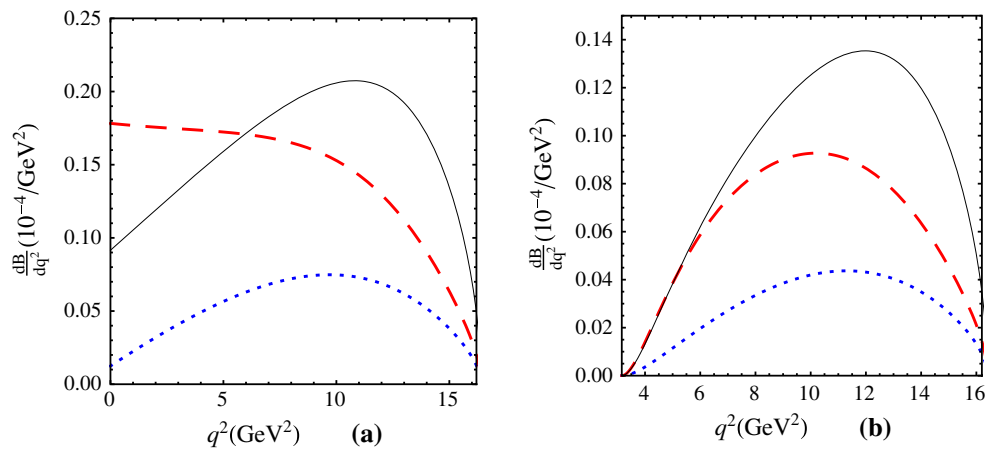


Fig. 3 Differential branching fractions $d\mathcal{B}/dq^2$ (in units of $10^{-4}/\text{GeV}^2$) for the decay $\bar{B}^0 \rightarrow a_1^+ \ell^- \bar{\nu}$. The left panel corresponds to $\ell = (e, \mu)$ and the right panel corresponds to $\ell = \tau$. The dotted, dashed and solid curves are obtained using the form factors calculated in LFQM, LCSR, and PQCD approach

Table 2 Integrated branching ratios for the $\bar{B}^0 \rightarrow a_1^+(1260)\ell^- \bar{\nu}$ decays (in units of 10^{-4}) with the form factors from the LFQM [14], LCSR [15] and PQCD [16]

$\ell = (e, \mu)$	\mathcal{B}_L	\mathcal{B}_T	$\mathcal{B}_{\text{total}}$	$\mathcal{B}_L/\mathcal{B}_T$	$\ell = \tau$	\mathcal{B}_L	\mathcal{B}_T	$\mathcal{B}_{\text{total}}$	$\mathcal{B}_L/\mathcal{B}_T$
LFQM	0.22	0.65	0.87	0.33	LFQM	0.09	0.28	0.38	0.33
LCSR	$0.74^{+0.31}_{-0.26}$	$1.60^{+0.66}_{-0.54}$	$2.34^{+0.97}_{-0.80}$	0.46	LCSR	$0.16^{+0.06}_{-0.05}$	$0.67^{+0.28}_{-0.23}$	$0.83^{+0.34}_{-0.28}$	0.24
PQCD	$1.42^{+0.99}_{-0.72}$	$1.21^{+0.71}_{-0.50}$	$2.63^{+1.71}_{-1.21}$	1.17	PQCD	$0.61^{+0.42}_{-0.31}$	$0.58^{+0.34}_{-0.24}$	$1.19^{+0.77}_{-0.54}$	1.05

Integrating over the q^2 , one obtains the longitudinal and transverse contributions to branching fractions of $\bar{B}^0 \rightarrow a_1^+ \ell^- \bar{\nu}$ decays, and our results are given in Table 2. Uncertainties shown in the table arise from the ones in the $B \rightarrow a_1$ form factors. We can see from this table that branching fractions for the $\bar{B}^0 \rightarrow a_1^+ \ell^- \bar{\nu}$ are of the order 10^{-4} . These values are comparable to the data by Belle collaboration on branching fractions for the semileptonic B decays into a vector meson [34]:

$$\mathcal{B}(B^- \rightarrow \rho^0 \ell^- \bar{\nu}) = (1.83 \pm 0.10 \pm 0.10) \times 10^{-4}, \quad (15)$$

$$\mathcal{B}(\bar{B}^0 \rightarrow \rho^+ \ell^- \bar{\nu}) = (3.22 \pm 0.27 \pm 0.24) \times 10^{-4}, \quad (16)$$

$$\mathcal{B}(B^- \rightarrow \omega \ell^- \bar{\nu}) = (1.07 \pm 0.16 \pm 0.07) \times 10^{-4}. \quad (17)$$

Babar collaboration [35] also gives similar results for the $B^- \rightarrow \omega \ell^- \bar{\nu}$:

$$\mathcal{B}(B^- \rightarrow \omega \ell^- \bar{\nu}) = (1.19 \pm 0.16 \pm 0.09) \times 10^{-4}. \quad (18)$$

Currently, there is no experimental analysis of the $\bar{B}^0 \rightarrow a_1(1260)^+ \ell^- \bar{\nu}$, but the two B factories at KEK and SLAC have accumulated about 10^9 events of B^0 and B^\pm . The branching fractions $\mathcal{O}(10^{-4})$ correspond to about 10^5 events for the signal. The above estimate may be affected by the detector efficiency, but an experimental search would very presumably lead to the observation of this decay mode. In addition, sizable branching fractions as shown in Table 2 also

indicate a promising prospect at the ongoing LHC experiment [36], the forthcoming Super-KEKB factory [37] and the under-design Circular Electron-Positron Collider (CEPC) [38].

2.3 Nonleptonic B decays into a_1

Since our main goal in this work is to investigate the internal structure of the $a_1(1420)$, we will focus on the decay modes which can be handled under the factorization approach. These decay modes are typically dominated by tree operators with effective Hamiltonian

$$\begin{aligned} \mathcal{H}_{\text{eff}} = & \frac{G_F}{\sqrt{2}} V_{Qb} V_{Q'd}^* \{ C_1 [\bar{Q}_\alpha \gamma^\mu (1 - \gamma_5) b_\beta] \\ & \times [\bar{d}_\beta \gamma_\mu (1 - \gamma_5) Q'_\alpha] + C_2 [\bar{Q}_\alpha \gamma^\mu (1 - \gamma_5) b_\alpha] \\ & \times [\bar{d}_\beta \gamma_\mu (1 - \gamma_5) Q'_\beta] \}, \end{aligned} \quad (19)$$

where C_1 and C_2 are the Wilson coefficients. The α and β are the color indices. Here $Q = u, c$ and $Q' = u, c$ denote the up type quarks. V_{ub}, V_{cb}, V_{ud} , and V_{cd} are the corresponding CKM matrix elements.

With the definitions of decay constants,

$$\begin{aligned} \langle a_1(p, \epsilon) | \bar{d} \gamma_\mu \gamma_5 u | 0 \rangle &= i f_{a_1} m_{a_1} \epsilon_\mu^*, \\ \langle J/\psi(p, \epsilon) | \bar{c} \gamma_\mu c | 0 \rangle &= f_{J/\psi} m_{J/\psi} \epsilon_\mu^*, \\ \langle \pi^-(p) | \bar{d} \gamma_\mu \gamma_5 u | 0 \rangle &= -i f_\pi p_\mu, \end{aligned} \quad (20)$$

we expect the factorization formula to have the form

$$i\mathcal{A}(\bar{B}^0 \rightarrow D^+ a_1^-) = (-i)^2 \frac{G_F}{\sqrt{2}} V_{cb} V_{ud}^* a_1 f_{a_1} F_1^{B \rightarrow D}(m_{a_1}^2) \times m_B^2 \sqrt{\lambda(1, r_D^2, r_{a_1}^2)}, \tag{21}$$

$$i\mathcal{A}(\bar{B}^0 \rightarrow \pi^+ a_1^-) = (-i)^2 \frac{G_F}{\sqrt{2}} V_{ub} V_{ud}^* a_1 f_{a_1} F_1^{B \rightarrow \pi}(m_{a_1}^2) \times m_B^2 \sqrt{\lambda(1, r_\pi^2, r_{a_1}^2)}, \tag{22}$$

$$i\mathcal{A}(\bar{B}^0 \rightarrow \pi^- a_1^+) = (-i)^2 \frac{G_F}{\sqrt{2}} V_{ub} V_{ud}^* a_1 f_\pi V_0^{B \rightarrow a_1}(m_\pi^2) \times m_B^2 \sqrt{\lambda(1, r_\pi^2, r_{a_1}^2)}, \tag{23}$$

$$i\mathcal{A}_L(\bar{B}^0 \rightarrow D^{*+} a_1^-) = \frac{(-i)^3 G_F}{\sqrt{2}} V_{cb} V_{ud}^* a_1 f_{a_1} m_B^2 \frac{1}{2r_{D^*}} \times \left[(1 - r_{D^*}^2 - r_{a_1}^2)(1 + r_{D^*}) A_1^{B \rightarrow D^*}(m_{a_1}^2) - \frac{\lambda(1, r_{D^*}^2, r_{a_1}^2)}{1 + r_{D^*}} A_2^{B \rightarrow D^*}(m_{a_1}^2) \right],$$

$$i\mathcal{A}_N(\bar{B}^0 \rightarrow D^{*+} a_1^-) = \frac{(-i)^3 G_F}{\sqrt{2}} V_{cb} V_{ud}^* a_1 f_{a_1} m_B^2 (1 + r_{D^*}) r_{a_1} A_1^{B \rightarrow D^*}(m_{a_1}^2),$$

$$i\mathcal{A}_T(\bar{B}^0 \rightarrow D^{*+} a_1^-) = \frac{-i G_F}{\sqrt{2}} V_{cb} V_{ud}^* a_1 f_{a_1} r_{a_1} m_B^2 \times \frac{\sqrt{\lambda(1, r_{a_1}^2, r_{D^*}^2)}}{(1 + r_{D^*})} V^{B \rightarrow D^*}(m_{a_1}^2), \tag{24}$$

$$i\mathcal{A}_L(B^- \rightarrow a_1^- J/\psi) = \frac{(-i)^3 G_F}{\sqrt{2}} V_{cb} V_{cd}^* a_2 f_{J/\psi} m_B^2 \frac{1}{2r_{a_1}} \times \left[(1 - r_{J/\psi}^2 - r_{a_1}^2)(1 - r_{a_1}) V_1^{B \rightarrow a_1}(m_{J/\psi}^2) - \frac{\lambda(1, r_{J/\psi}^2, r_{a_1}^2)}{1 - r_{a_1}} V_2^{B \rightarrow a_1}(m_{J/\psi}^2) \right],$$

$$i\mathcal{A}_N(B^- \rightarrow a_1^- J/\psi) = \frac{(-i)^3 G_F}{\sqrt{2}} V_{cb} V_{cd}^* a_2 f_{J/\psi} m_B^2 r_{J/\psi} \times (1 - r_{a_1}) V_1^{B \rightarrow a_1}(m_{J/\psi}^2),$$

$$i\mathcal{A}_T(B^- \rightarrow a_1^- J/\psi) = \frac{-i G_F}{\sqrt{2}} V_{cb} V_{cd}^* a_2 f_{J/\psi} m_B^2 r_{J/\psi} \times \frac{\sqrt{\lambda(1, r_{J/\psi}^2, r_{a_1}^2)}}{1 - r_{a_1}} A^{B \rightarrow a_1}(m_{J/\psi}^2), \tag{25}$$

with $a_1 = C_2 + C_1/N_c$ and $a_2 = C_1 + C_2/N_c$ ($N_c = 3$). In the above, the amplitude for the $B \rightarrow J/\psi a_1$ has been decomposed according to the Lorentz structures

$$\mathcal{A} = \mathcal{A}_L + \epsilon_{J/\psi}^*(T) \cdot \epsilon_{a_1}^*(T) \mathcal{A}_N + i\mathcal{A}_T \epsilon_{\alpha\beta\gamma\rho} \epsilon_{J/\psi}^{*\alpha} \epsilon_{a_1}^{*\beta}$$

$$\times \frac{2P_{J/\psi}^\gamma P_{a_1}^\rho}{\sqrt{\lambda(m_B^2, m_{J/\psi}^2, m_{a_1}^2)}}. \tag{26}$$

The partial decay width of the $B \rightarrow a_1 P$, where P denotes a pseudoscalar meson, is given as

$$\Gamma(B \rightarrow a_1 P) = \frac{|\vec{p}|}{8\pi m_B^2} |\mathcal{A}(B \rightarrow a_1 P)|^2, \tag{27}$$

with $|\vec{p}|$ being the three-momentum of the a_1 in the B meson rest frame. For the $B \rightarrow a_1 V$, the partial decay width is the summation of three polarizations,

$$\Gamma(B \rightarrow a_1 V) = \frac{|\vec{p}|}{8\pi m_B^2} (|\mathcal{A}_0(B \rightarrow a_1 V)|^2 + 2|\mathcal{A}_N(B \rightarrow a_1 V)|^2 + 2|\mathcal{A}_T(B \rightarrow a_1 V)|^2). \tag{28}$$

We use the LFQM results [14] for all transition form factors and the other inputs are given as [2]

$$\tau_{B^-} = (1.638 \times 10^{-12})s, \quad \tau_{B_s} = (1.511 \times 10^{-12})s \tag{29}$$

$$|V_{cb}| = 41.1 \times 10^{-3}, \quad |V_{ud}| = 0.974, \quad |V_{cd}| = 0.225, \tag{30}$$

The f_π and $f_{J/\psi}$ can be extracted from the $\pi^- \rightarrow \ell^- \bar{\nu}$ and $J/\psi \rightarrow \ell^+ \ell^-$ data [2]:

$$f_\pi = 130.4 \text{ MeV}, \quad f_{J/\psi} = (416.3 \pm 5.3) \text{ MeV}. \tag{31}$$

We use QCD sum rules results for the f_{a_1} [39]

$$f_{a_1} = (238 \pm 10) \text{ MeV}. \tag{32}$$

It is necessary to stress that the Wilson coefficients are scale dependent which give rise to some uncertainties to our theoretical predictions. Fortunately, the scale dependence in a_1 is less severe, for instance, the leading order results with α_s in NLO will be changed from 1.024 to 1.086 when the scale runs from 5.0 to 1.5 GeV [40]. This will introduce at most about 10 % to branching ratios, which are smaller than hadronic uncertainties in most cases. In the following, we will use the value corresponding to the typical factorization scale $\mu \sim \sqrt{\Lambda_{\text{QCD}} m_B} \sim 1.7 \text{ GeV}$ [40],

$$a_1 = 1.07. \tag{33}$$

The situation is complicated for the Wilson coefficient a_2 . First this coefficient has a significant scale dependence [40]. Second, after incorporating the sizable higher order QCD corrections, the effective a_2 becomes complex. In this work, we will assume that this quantity is the same for the $B \rightarrow J/\psi K^*$ and $B \rightarrow J/\psi a_1$. Then we can make use of the data on the $B \rightarrow J/\psi K^*$ data [2] to extract its module:

$$|a_2| = (0.234 \pm 0.006). \tag{34}$$

As a result our theoretical results for branching ratios are given as

$$\mathcal{B}(\bar{B}^0 \rightarrow D^+ a_1^-) = (1.3 \pm 0.1) \%, \tag{35}$$

$$\mathcal{B}(\bar{B}^0 \rightarrow \pi^+ a_1^-) = (1.9 \pm 0.2) \times 10^{-5}, \tag{36}$$

$$\mathcal{B}(\bar{B}^0 \rightarrow D^{*+} a_1^-) = (1.6 \pm 0.2) \%, \tag{37}$$

where the errors come from the one in the f_{a_1} . For decay modes induced by the $B \rightarrow a_1$ transition, we have

$$\mathcal{B}(\bar{B}^0 \rightarrow \pi^- a_1^+) = \begin{cases} 0.13 \times 10^{-5}, & \text{LFQM} \\ (0.70^{+0.25}_{-0.22}) \times 10^{-5}, & \text{LCSR,} \\ (0.89^{+0.68}_{-0.48}) \times 10^{-5}, & \text{PQCD,} \end{cases} \tag{38}$$

$$\mathcal{B}(B^- \rightarrow a_1^- J/\psi) = \begin{cases} 3.6 \times 10^{-5}, & \text{LFQM} \\ (7.5^{+3.1}_{-2.5}) \times 10^{-5}, & \text{LCSR,} \\ (9.8^{+6.3}_{-4.4}) \times 10^{-5}, & \text{PQCD,} \end{cases} \tag{39}$$

where the errors arise from those in form factors.

The Babar [41] and Belle [42] collaborations have reported the observation of $B^0 \rightarrow a_1^\pm \pi^\mp$ and their results for the branching fractions are given as

$$\begin{aligned} &\mathcal{B}(\bar{B}^0 \rightarrow \pi^\pm a_1^\mp) \mathcal{B}(a_1^\pm \rightarrow \pi^\pm \pi^\mp \pi^\pm) \\ &= \begin{cases} (16.6 \pm 1.9 \pm 1.5) \times 10^{-6}, & \text{Babar,} \\ (11.1 \pm 1.0 \pm 1.4) \times 10^{-6}, & \text{Belle.} \end{cases} \end{aligned} \tag{40}$$

The above results have been averaged by the PDG as [2]

$$\mathcal{B}(\bar{B}^0 \rightarrow \pi^\pm a_1^\mp) = (2.6 \pm 0.5) \times 10^{-5}. \tag{41}$$

As we can see, the averaged data is consistent with our theoretical results in Eqs. (38) and (39).

We also predict the branching ratios for $\bar{B}_s^0 \rightarrow D_s^+ a_1^-$ and $\bar{B}_s^0 \rightarrow D_s^{*+} a_1^-$:

$$\mathcal{B}(\bar{B}_s^0 \rightarrow D_s^+ a_1^-) = (1.3 \pm 0.1) \%. \tag{42}$$

$$\mathcal{B}(\bar{B}_s^0 \rightarrow D_s^{*+} a_1^-) = (1.7 \pm 0.2) \%. \tag{43}$$

The numerical results given in Eqs. (35)–(43) indicate that there is a promising prospect to study these decays by the LHCb, Babar, and Belle collaborations, and on the forthcoming Super-KEKB factory and the CEPC.

3 $D \rightarrow a_1$ decays

By replacing the corresponding form factors and CKM matrix elements, the analysis of B decays in the last section can be straightforwardly generalized to the $D \rightarrow a_1$ decays. The $D \rightarrow a_1$ form factors are only available in LFQM [14] and we summarize these results in Table 3. We will use other input parameters as follows [2]:

$$m_{D^0} = 1.8648 \text{ GeV}, \quad |V_{cd}| = 0.225,$$

Table 3 The $D \rightarrow a_1$ form factors calculated in the covariant LFQM [14]

F	$F(0)$	a	b
$A^{D \rightarrow a_1}$	0.20	0.98	0.20
$V_0^{D \rightarrow a_1}$	0.31	0.85	0.49
$V_1^{D \rightarrow a_1}$	1.54	-0.05	0.05
$V_2^{D \rightarrow a_1}$	0.06	0.12	0.10

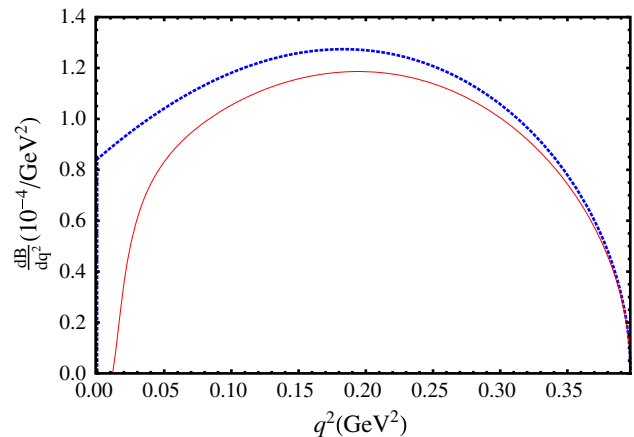


Fig. 4 Differential branching fractions $d\mathcal{B}/dq^2$ (in units of $10^{-4}/\text{GeV}^2$) for the decay $D^0 \rightarrow a_1^- \ell^+ \nu$. The dotted and solid curve corresponds to $\ell = e$ and $\ell = \mu$, respectively. The differences between the two curves arise from the lepton masses and can reach about 10 %

Table 4 Integrated branching ratios for the $D^0 \rightarrow a_1^-(1260)\ell^+\nu$ decays (in units of 10^{-4})

	\mathcal{B}_L	\mathcal{B}_T	$\mathcal{B}_{\text{total}}$	$\mathcal{B}_L/\mathcal{B}_T$
$\ell = e$	0.21	0.20	0.41	1.05
$\ell = \mu$	0.18	0.18	0.36	1.00

$$\tau_{D^0} = 0.410 \times 10^{-12} \text{ s}, \quad \tau_{D_s} = 0.500 \times 10^{-12} \text{ s}. \tag{44}$$

Our results for the differential branching ratios of the semileptonic $D^0 \rightarrow a_1^- \ell^+ \nu$ are given in Fig. 4, and the integrated branching fractions are presented in Table 4. In Fig. 4, the dotted and solid curve corresponds to $\ell = e$ and $\ell = \mu$, respectively. The differences in the two curves arise from the lepton masses and can reach about 10 %.

Recently, based on the 2.9 fb^{-1} data of electron–positron annihilation data collected at a center-of-mass energy of $\sqrt{s} = 3.773 \text{ GeV}$, BES-III collaboration has searched for the $D^+ \rightarrow \omega \ell^+ \nu$ decay [43] and the branching fraction is measured

$$\mathcal{B}(D^+ \rightarrow \omega \ell^+ \nu) = (1.63 \pm 0.11 \pm 0.08) \times 10^{-3}. \tag{45}$$

In this procedure, the ω meson is reconstructed by three pions, and it is interesting to notice that the neutral $a_1(1260)$

should also be reconstructed by the same final state. Extending the analysis in Ref. [43] to higher mass region at round 1.23 GeV may discover the $D^+ \rightarrow a_1^0 \ell^+ \nu$ transition. Actually, BES-III have collected about 10^7 events of $D - \bar{D}$. The 10^{-4} branching fractions correspond to about 10^3 events for the $D \rightarrow a_1 \ell^+ \nu$, which might be observed in the future analysis.

We can also study the nonleptonic D/D_s decays into $a_1(1260)$ with the factorization amplitudes:

$$i\mathcal{A}(D^0 \rightarrow a_1^+ \pi^-) = (-i)^2 \frac{G_F}{\sqrt{2}} V_{cd}^* V_{ud} a_1 f_{a_1} F_1^{D \rightarrow \pi}(m_{a_1}^2) \times \sqrt{\lambda(m_D^2, m_\pi^2, m_{a_1}^2)}, \tag{46}$$

$$i\mathcal{A}(D^0 \rightarrow \pi^+ a_1^-) = (-i)^2 \frac{G_F}{\sqrt{2}} V_{cd}^* V_{ud} a_1 f_\pi V_0^{D \rightarrow a_1}(m_\pi^2) \times \sqrt{\lambda(m_D^2, m_\pi^2, m_{a_1}^2)}, \tag{47}$$

$$i\mathcal{A}(D_s^+ \rightarrow a_1^+ K^0) = (-i)^2 \frac{G_F}{\sqrt{2}} V_{cd}^* V_{ud} a_1 f_{a_1} F_1^{D_s \rightarrow K}(m_{a_1}^2) \times \sqrt{\lambda(m_{D_s}^2, m_K^2, m_{a_1}^2)}, \tag{48}$$

where the Wilson coefficient a_1 at a lower scale should be used. For instance, the value at $\mu = 1$ GeV, $a_1 = 1.14$, is about 7 % larger than the one used in B decays [40]. In this case, our theoretical results are given as

$$\mathcal{B}(D^0 \rightarrow a_1^+ \pi^-) = (4.7 \pm 0.5) \times 10^{-3}, \tag{49}$$

$$\mathcal{B}(D^0 \rightarrow \pi^+ a_1^-) = 9.3 \times 10^{-5}, \tag{50}$$

$$\mathcal{B}(D_s^+ \rightarrow a_1^+ K^0) = (2.6 \pm 0.3) \times 10^{-3}, \tag{51}$$

where the errors arise from those in the decay constant f_{a_1} .

The FOCUS collaboration has measured the branching fraction for the $D^0 \rightarrow a_1^\pm \pi^\mp$ [44]:

$$\mathcal{B}(D^0 \rightarrow a_1^\pm \pi^\mp) = (4.47 \pm 0.32) \times 10^{-3}, \tag{52}$$

which is consistent with our theoretical results in Eqs. (49) and (50). The LHCb collaboration makes use of the $D^0 \rightarrow a_1^\pm \pi^\mp$ to study CP violation [45], and it is also feasible to study this mode using the CLEO-c data [46]. The BES-III collaboration has accumulated about 10^7 events of the D^0 and will collect about 3 fb^{-1} data at the center-of-mass $\sqrt{s} = 4.17$ GeV to produce the $D_s^+ D_s^-$ [47, 48]. All these data can be used to study the charm decays into the a_1 .

4 Conclusions

Experimental observations of resonance-like states in recent years have invoked theoretical research interest on exotic hadron spectroscopy. In particular, many of the established structures defy the naive quark model assignment as a $\bar{q}q$ or qqq state. At the low-energy, the $a_1(1420)$ with $I^G(J^{PC}) = 1^-(1^{++})$ observed in the $\pi^+ f_0(980)$ final state

in the $\pi^- p \rightarrow \pi^+ \pi^- \pi^- p$ process by COMPASS collaboration seems unlikely to be an ordinary $\bar{q}q$ mesonic state. Available theoretical explanations include tetraquark or rescattering effects due to $a_1(1260)$ decays. If the $a_1(1420)$ were induced by rescattering effects, its production rates are completely determined by those of the $a_1(1260)$.

In this work, we have studied various decays of heavy B/D mesons into the $a_1(1260)$, based on the form factors derived in different approaches. These decay modes are helpful to explore the dynamics in heavy to light transitions. We have also proposed to study the ratios of branching fractions of decays into the $a_1(1420)$ and $a_1(1260)$, and testing the universality of these ratios would be a straightforward way to validate/invalidate the rescattering explanation. The decay modes include in the charm sector the $D^0 \rightarrow a_1^- \ell^+ \nu$ and $D \rightarrow \pi^\pm a_1^\mp$, and in the bottom sector $B \rightarrow a_1 \ell \bar{\nu}$ and $B \rightarrow Da_1, \pi^\pm a_1^\mp$, and the $B_c \rightarrow J/\psi a_1$ and $\Lambda_b \rightarrow \Lambda_c a_1$. We have calculated the branching ratios for various decays into the $a_1(1260)$. Other decay modes like $\Lambda_b \rightarrow \Lambda_c a_1$ and $B_c^- \rightarrow J/\psi a_1^-$, measured by the LHCb collaboration [49] and CMS collaboration [50], in agreement with theoretical results based on the form factors [51, 52], are also of helpful in this aspect.

Our results have indicated that there is a promising prospect to study these decays on experiments including BES-III, LHCb, Babar, Belle and CLEO-c, the forthcoming Super-KEKB factory and the under-design Circular Electron-Positron Collider. Experimental analyses in future will very probably lead to a deeper understanding of the nature of the $a_1(1420)$.

Acknowledgments The authors are grateful to Prof. Hai-bo Li, Dr. Jian-Ping Dai, and Yong Huang for enlightening discussions. This work was supported in part by National Natural Science Foundation of China under Grant No. 11575110, Natural Science Foundation of Shanghai under Grant Nos. 11DZ2260700, 15DZ2272100, and No. 15ZR1423100, by the Open Project Program of State Key Laboratory of Theoretical Physics, Institute of Theoretical Physics, Chinese Academy of Sciences, China (No. Y5KF111CJ1), and by Scientific Research Foundation for Returned Overseas Chinese Scholars, State Education Ministry.

Open Access This article is distributed under the terms of the Creative Commons Attribution 4.0 International License (<http://creativecommons.org/licenses/by/4.0/>), which permits unrestricted use, distribution, and reproduction in any medium, provided you give appropriate credit to the original author(s) and the source, provide a link to the Creative Commons license, and indicate if changes were made. Funded by SCOAP³.

References

1. M. Gell-Mann, Phys. Lett. **8**, 214 (1964). doi:10.1016/S0031-9163(64)92001-3
2. K.A. Olive et al. (Particle Data Group Collaboration), Chin. Phys. C **38**, 090001 (2014). doi:10.1088/1674-1137/38/9/090001

3. S.K. Choi et al. (Belle Collaboration), *Phys. Rev. Lett.* **91**, 262001 (2003). doi:10.1103/PhysRevLett.91.262001. arXiv:hep-ex/0309032
4. S.K. Choi et al. (Belle Collaboration), *Phys. Rev. Lett.* **100**, 142001 (2008). doi:10.1103/PhysRevLett.100.142001. arXiv:0708.1790 [hep-ex]
5. A. Bondar et al. (Belle Collaboration), *Phys. Rev. Lett.* **108**, 122001 (2012). doi:10.1103/PhysRevLett.108.122001. arXiv:1110.2251 [hep-ex]
6. M. Ablikim et al. (BESIII Collaboration), *Phys. Rev. Lett.* **110**, 252001 (2013). doi:10.1103/PhysRevLett.110.252001. arXiv:1303.5949 [hep-ex]
7. Z.Q. Liu et al. (Belle Collaboration), *Phys. Rev. Lett.* **110**, 252002 (2013). doi:10.1103/PhysRevLett.110.252002. arXiv:1304.0121 [hep-ex]
8. T. Xiao, S. Dobbs, A. Tomaradze, K.K. Seth, *Phys. Lett. B* **727**, 366 (2013). doi:10.1016/j.physletb.2013.10.041. arXiv:1304.3036 [hep-ex]
9. R. Aaij et al. (LHCb Collaboration), *Phys. Rev. Lett.* **115**, 072001 (2015). doi:10.1103/PhysRevLett.115.072001. arXiv:1507.03414 [hep-ex]
10. N. Brambilla et al., *Eur. Phys. J. C* **71**, 1534 (2011). doi:10.1140/epjc/s10052-010-1534-9. arXiv:1010.5827 [hep-ph]
11. K. Abe et al. (Belle Collaboration), *Phys. Rev. Lett.* **87**, 161601 (2001). doi:10.1103/PhysRevLett.87.161601. arXiv:hep-ex/0105014
12. B. Aubert et al. (BaBar Collaboration), arXiv:hep-ex/0207085
13. Y. Amhis et al. (Heavy Flavor Averaging Group (HFAG) Collaboration), arXiv:1412.7515 [hep-ex]
14. H.Y. Cheng, C.K. Chua, C.W. Hwang, *Phys. Rev. D* **69**, 074025 (2004). doi:10.1103/PhysRevD.69.074025. arXiv:hep-ph/0310359
15. K.C. Yang, *Phys. Rev. D* **78**, 034018 (2008). doi:10.1103/PhysRevD.78.034018. arXiv:0807.1171 [hep-ph]
16. R.H. Li, C.D. Lu, W. Wang, *Phys. Rev. D* **79**, 034014 (2009). doi:10.1103/PhysRevD.79.034014. arXiv:0901.0307 [hep-ph]
17. R.C. Verma, *J. Phys. G* **39**, 025005 (2012). doi:10.1088/0954-3889/39/2/025005. arXiv:1103.2973 [hep-ph]
18. S. Yan-Jun, W. Zhi-Gang, H. Tao, *Chin. Phys. C* **36**, 1046 (2012). doi:10.1088/1674-1137/36/11/003. arXiv:1106.4915 [hep-ph]
19. D. Ebert, R.N. Faustov, V.O. Galkin, *Phys. Rev. D* **85**, 054006 (2012). doi:10.1103/PhysRevD.85.054006. arXiv:1107.1988 [hep-ph]
20. Z.G. Wang, *Phys. Lett. B* **666**, 477 (2008). doi:10.1016/j.physletb.2008.08.014. arXiv:0804.0907 [hep-ph]
21. F. Najafi, H. Mehraban, *PTEP* **2015**(3), 033B09 (2015). doi:10.1093/ptep/ptv001. arXiv:1412.7951 [hep-ph]
22. Z.Q. Zhang, arXiv:1203.5913 [hep-ph]
23. X. Liu, Z.J. Xiao, *Phys. Rev. D* **86**, 074016 (2012). doi:10.1103/PhysRevD.86.074016. arXiv:1203.6135 [hep-ph]
24. Z.Q. Zhang, *Phys. Rev. D* **87**(7), 074030 (2013). doi:10.1103/PhysRevD.87.074030
25. H.Y. Cheng, C.W. Chiang, *Phys. Rev. D* **81**, 074031 (2010). doi:10.1103/PhysRevD.81.074031. arXiv:1002.2466 [hep-ph]
26. C. Adolph et al. (COMPASS Collaboration), *Phys. Rev. Lett.* **115**(8), 082001 (2015). doi:10.1103/PhysRevLett.115.082001. arXiv:1501.05732 [hep-ex]
27. B. Ketzner (COMPASS Collaboration), *PoS Hadron* **2013**, 011 (2013). arXiv:1403.4884 [hep-ex]
28. Y. Khokhlov et al., *PoS Hadron* **2013**, 088 (2013)
29. H.X. Chen, E.L. Cui, W. Chen, T.G. Steele, X. Liu, S.L. Zhu, *Phys. Rev. D* **91**, 094022 (2015). doi:10.1103/PhysRevD.91.094022. arXiv:1503.02597 [hep-ph]
30. M. Mikhasenko, B. Ketzner, A. Sarantsev, *Phys. Rev. D* **91**(9), 094015 (2015). doi:10.1103/PhysRevD.91.094015. arXiv:1501.07023 [hep-ph]
31. X.H. Liu, M. Oka, Q. Zhao, *Phys. Lett. B* **753**, 297 (2016). doi:10.1016/j.physletb.2015.12.027. arXiv:1507.01674 [hep-ph]
32. W. Wang, *Int. J. Mod. Phys. A* **29**, 1430040 (2014). doi:10.1142/S0217751X14300403. arXiv:1407.6868 [hep-ph]
33. G. Ricciardi, arXiv:1412.4288 [hep-ph]
34. A. Sibidanov et al. (Belle Collaboration), *Phys. Rev. D* **88**(3), 032005 (2013). doi:10.1103/PhysRevD.88.032005. arXiv:1306.2781 [hep-ex]
35. J.P. Lees et al. (BaBar Collaboration), *Phys. Rev. D* **86**, 092004 (2012). doi:10.1103/PhysRevD.86.092004. arXiv:1208.1253 [hep-ex]
36. R. Aaij et al. (LHCb Collaboration), *Eur. Phys. J. C* **73**(4), 2373 (2013). doi:10.1140/epjc/s10052-013-2373-2. arXiv:1208.3355 [hep-ex]
37. T. Aushev et al. arXiv:1002.5012 [hep-ex]
38. The preliminary Conceptual Design Report can be found at: http://cepc.ihep.ac.cn/preCDR/main_preCDR
39. K.C. Yang, *Nucl. Phys. B* **776**, 187 (2007). doi:10.1016/j.nuclphysb.2007.03.046. arXiv:0705.0692 [hep-ph]
40. G. Buchalla, A.J. Buras, M.E. Lautenbacher, *Rev. Mod. Phys.* **68**, 1125 (1996). doi:10.1103/RevModPhys.68.1125. arXiv:hep-ph/9512380
41. B. Aubert et al. (BaBar Collaboration), *Phys. Rev. Lett.* **97**, 051802 (2006). doi:10.1103/PhysRevLett.97.051802. arXiv:hep-ex/0603050
42. J. Dalseno et al. (Belle Collaboration), *Phys. Rev. D* **86**, 092012 (2012). doi:10.1103/PhysRevD.86.092012. arXiv:1205.5957 [hep-ex]
43. M. Ablikim et al. (BESIII Collaboration), *Phys. Rev. D* **92**(7), 071101 (2015). doi:10.1103/PhysRevD.92.071101. arXiv:1508.00151 [hep-ex]
44. J.M. Link et al. (FOCUS Collaboration), *Phys. Rev. D* **75**, 052003 (2007). doi:10.1103/PhysRevD.75.052003. arXiv:hep-ex/0701001
45. R. Aaij et al. (LHCb Collaboration), *Phys. Lett. B* **726**, 623 (2013). doi:10.1016/j.physletb.2013.09.011. arXiv:1308.3189 [hep-ex]
46. J. Benton, arXiv:1312.3821 [hep-ex]
47. M. Ablikim et al. (BESIII Collaboration), *Phys. Rev. D* **89**(5), 052001 (2014). doi:10.1103/PhysRevD.89.052001. arXiv:1401.3083 [hep-ex]
48. D.M. Asner et al., *Int. J. Mod. Phys. A* **24**, S1 (2009). arXiv:0809.1869 [hep-ex]
49. R. Aaij et al. (LHCb Collaboration), *Phys. Rev. Lett.* **108**, 251802 (2012). doi:10.1103/PhysRevLett.108.251802. arXiv:1204.0079 [hep-ex]
50. V. Khachatryan et al. (CMS Collaboration), *JHEP* **1501**, 063 (2015). doi:10.1007/JHEP01(2015)063. arXiv:1410.5729 [hep-ex]
51. W. Wang, Y.L. Shen, C.D. Lu, *Phys. Rev. D* **79**, 054012 (2009). doi:10.1103/PhysRevD.79.054012. arXiv:0811.3748 [hep-ph]
52. A.K. Likhoded, A.V. Luchinsky, *Phys. Rev. D* **81**, 014015 (2010). doi:10.1103/PhysRevD.81.014015. arXiv:0910.3089 [hep-ph]